

Tunable diffraction grating using ultraviolet-light-induced spatial phase modulation in dual-frequency liquid crystal

Pao-Tai Lin, Xiao Liang, Hongwen Ren, and Shin-Tson Wu^{a)}

College of Optics and Photonics, University of Central Florida, Orlando, Florida 32816

(Received 12 April 2004; accepted 22 June 2004)

An electrically tunable diffraction phase grating using ultraviolet (UV)-light-induced spatial dielectric modulation of a dual-frequency liquid crystal (DFLC) cell is demonstrated. A photomask with transparent and opaque stripes was used for fabricating the grating. In the UV-exposed stripes, the negative dielectric anisotropy ($\Delta\epsilon$) tolane compound of the DFCL mixture is partially polymerized resulting in a decreased threshold voltage as compared to that of the unexposed region. Upon applying a constant voltage, the phase difference between the adjacent pixels is produced. The first-order diffraction efficiency reaches $\sim 60\%$ which agrees well with the simulation results. Due to the dual-frequency addressing at $30 V_{\text{rms}}$, the response time of the DFCL phase grating was measured to be ~ 1 ms at room temperature. © 2004 American Institute of Physics.

[DOI: 10.1063/1.1781752]

Liquid crystal (LC) phase grating has been widely used for laser beam steering,¹ tunable-focus lens,² and foveated imaging.³ Two physical mechanisms have been commonly employed for demonstrating phase grating devices: A homogeneous LC layer with an inhomogeneous electric field, and an inhomogeneous LC layer with a homogeneous electric field. The former examples include optical phased arrays (OPAs) and the latter include alternative twisted-nematic domains,⁴ modulated Freedericksz transition threshold in dual-frequency LC material,⁵ and gradient refractive index nanoscale polymer-dispersed liquid crystal (GRIN PDLC) droplets.⁶ Each approach has its own pros and cons. An OPA exhibits a high diffraction efficiency and low operating voltage, however, its pixilated structure is sophisticated. On the other hand, the GRIN PDLC has a fast response time and is independent of polarization except that its phase change is small and the operating voltage is high ($>100 V_{\text{rms}}$). There is an urgent need to develop phase gratings with high diffraction efficiency, fast response time, and low operating voltage.

In this letter, we demonstrate a phase grating based on the spatial dielectric modulation of the dual-frequency liquid crystal (DFLC). For a DFCL, the dielectric anisotropy ($\Delta\epsilon$) is positive at low frequencies, gradually decreases to zero, and then becomes negative as the frequency increases.⁷ The frequency that $\Delta\epsilon=0$ is called cross-over frequency (f_c). In practice, a DFCL mixture is comprised of positive and negative $\Delta\epsilon$ LC compounds and its cross-over frequency is around a few kilohertz, depending on the molecular structures and compositions. The major attraction of the DFCL device is fast response time. During the turn-on and -off processes, ac voltage bursts with low and high frequencies are applied. As a result, fast rise and decay times are achieved. In our device, the phase grating is controlled by the UV exposure through a spatially alternating opaque and transparent photomask. With this simple design, the measured first-order (± 1) diffraction efficiency achieves $\sim 60\%$.

To fabricate the LC phase grating, we exposed UV ($\lambda \sim 365$ nm) light to the DFCL cell through a patterned pho-

tomask. The width of the alternating transparent stripe is $16 \mu\text{m}$ and the opaque stripe is $234 \mu\text{m}$. Figure 1(a) depicts the experimental setup. The photomask is in proximity contact with the LC cell. A high performance DFCL mixture consisting of biphenyl esters ($\Delta\epsilon \sim 30$) and laterally difluorotolanes ($\Delta\epsilon \sim -6$) has been recently reported.⁸ For proving principle, we used a binary DFCL mixture consisting of 20% biphenyl ester and 80% difluoro-tolane. Its cross-over frequency occurs at $f_c \sim 1.1$ kHz. The binary DFCL mixture was injected into a homogeneous cell with gap $d=7.7 \mu\text{m}$ by capillary flow. The transmitted UV light through the photomask generates free radicals around the carbon-carbon triple bonds of the difluoro tolane molecules and causes a partial polymerization.⁹ On the other hand, the biphenyl esters are inert to the UV irradiation because of their shorter molecular conjugation. The small reduction of the difluoro tolane composition causes the cross-over frequency to increase because

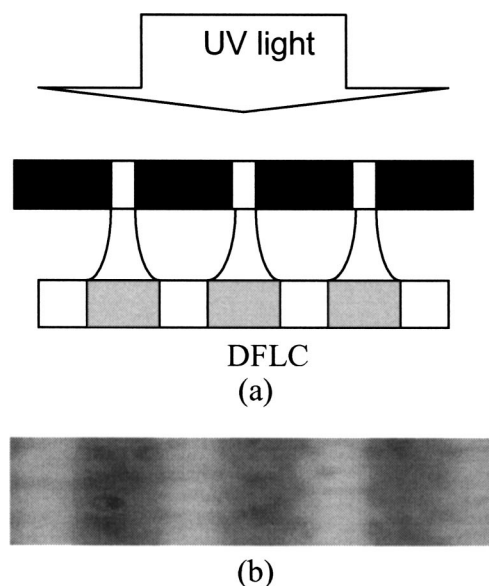


FIG. 1. (a) Experimental setup for fabricating DFCL phase grating. (b) Microscope image of the UV exposed DFCL through photomask. Polarizers are crossed.

^{a)}Electronic mail: swu@mail.ucf.edu

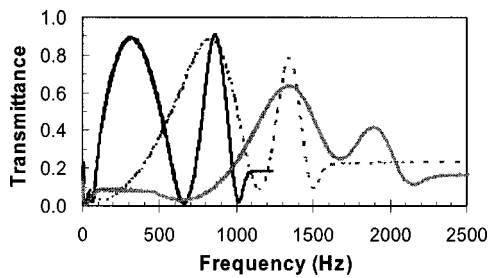


FIG. 2. Frequency-dependent transmittance of three DFCL cells with 0 (dark line), 200 s (gray), and 300 s (thin dark line) UV exposure time, respectively. The applied voltage is fixed at $15 V_{\text{rms}}$; $T=23^\circ\text{C}$ and $\lambda=633\text{ nm}$.

the mixture's $\Delta\epsilon$ becomes more positive in the low-frequency regime. Therefore, the exposed pixels exhibit a lower threshold voltage than the opaque ones. If we apply a constant low-frequency voltage to the DFCL cell, the transparent and opaque stripes will have a different phase difference. As a result, the diffraction effect would occur.

Figure 1(b) shows the microscope image of the exposed DFCL cell situated between crossed polarizers. Indeed, the exposed and unexposed stripes have different phase retardations. The transmitted UV light from the photomask is diffracted and after passing the top 1.1-mm-thick glass substrate, the beam is expanded by $\sim 5\times$.¹⁰ From Fig 1(b), the ratio of the unexposed and exposed stripes is $\alpha\sim 0.6$. This parameter will be used later for calculating the diffraction efficiency.

To examine how UV affects the cross-over frequency, we compare three DFCL samples; A, B, and C which correspond to 0, 200, and 300 s of UV exposures. In this study, no photomask was used. Figure 2 shows the frequency-dependent transmittance of these three samples. The applied voltage was fixed at $V=15 V_{\text{rms}}$ and the transmittance measured with a He-Ne laser ($\lambda=633\text{ nm}$) between two crossed polarizers at $T\sim 23^\circ\text{C}$. In the low-frequency regime, the DFCL has a positive $\Delta\epsilon$ so that the LC directors are reoriented by the electric field. As the frequency approaches f_c , the dielectric anisotropy gradually decreases which implies to an increased threshold voltage. In the $f\geq f_c$ regime, the low-frequency electric field can no longer reorient the LC directors because $\Delta\epsilon<0$. As a result, the transmittance remains flat. From Fig. 2, the cross-over frequency of the unexposed sample (dark line) is $f_c\sim 1.1\text{ kHz}$. As UV exposure time increases to 200 s (dashed lines) and 300 s (gray line), the cross-over frequency increases to 1.65 and 2.3 kHz, respectively. Due to this frequency shift, at $V=15 V_{\text{rms}}$ and $f=1\text{ kHz}$, the phase difference between samples A and C is $\delta\sim 3.7\pi$. This experiment proves that the phase difference between the exposed and unexposed areas can be controlled by the UV intensity and the applied voltage and frequency.

Based on the results obtained from Fig. 2, we fabricated a phase grating using a photomask shown in Fig. 1(a). At $V=30 V_{\text{rms}}$, the DFCL gratings have the highest diffraction efficiency. Since the homogeneous LC cell is uniaxial, only the extraordinary ray experiences the spatial phase retardation during molecular reorientation. Figure 3 plots the frequency-dependent normalized diffracted laser power of the DFCL samples with 200 s (left) and 300 s (right) UV exposures through photomask. Here, unity stands for the transmittance at $V=0$ where no diffraction occurs. The UV exposure time not only affects the cross-over frequency but

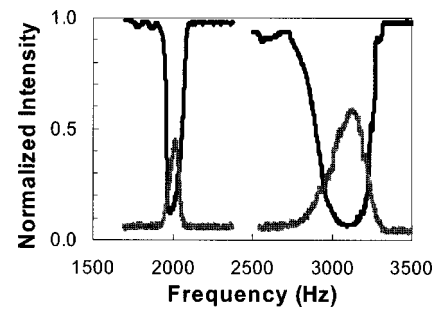


FIG. 3. Frequency-dependent diffracted HeNe laser power of the DFCL cell after 200 s (left) and 300 s (right) UV exposure through a photomask. The applied voltage is fixed at $30 V_{\text{rms}}$; $T=23^\circ\text{C}$ and $\lambda=633\text{ nm}$. Gray lines represent first-order diffractions.

also broadens its bandwidth. As the UV exposure increases from 200 to 300 s, more difluoro-tolane molecules are polymerized in the exposed stripes so that the cross-over frequency shifts from $\sim 1.9\text{ kHz}$ to 2.75 kHz . Moreover, its bandwidth is widened from $\sim 200\text{ Hz}$ to $\sim 500\text{ Hz}$. The measured first-order peak diffraction efficiency (gray lines) increases from 45% to 59%. For a longer UV exposure, more tolane molecules are polymerized and the LC alignment in the exposed pixels is disturbed. The former factor leads to an enlarged phase difference between the adjacent pixels and the latter suppresses the higher diffraction orders. The overall effect is that the first-order diffraction efficiency is improved. The response time of the DFCL gratings ($d=7.7\ \mu\text{m}$) with 200 s and 300 s UV exposures were measured to be $\sim 1\text{ ms}$ and 2 ms , respectively, when the frequency is switched from f_c to 50 kHz while keeping voltage at $V=30 V_{\text{rms}}$. As the voltage increases, the response time is faster, however, the diffraction efficiency gradually decreases.

The observed fast response is the key feature of a DFCL device. In the low-frequency regime, the DFCL has a positive $\Delta\epsilon$. The applied voltage (say $30 V_{\text{rms}}$) reorients the LC directors from a homogeneous to a homeotropic direction. During decay process, a high-frequency voltage is applied. Under such a circumstance, the $\Delta\epsilon$ becomes negative so that the applied electric field exerts a torque to assist the LCs relax back from a homeotropic to a homogeneous direction.

Figure 4 shows the diffraction patterns captured by a camera. The lower photo in Fig. 4(a) shows the input light while the top photo shows the diffraction patterns for the sample with 200 s UV exposure. Up to \pm fourth-diffraction orders are observed as the frequency gets close to f_c . Outside this region, diffraction does not occur. When $f>f_c$, the LC molecules do not respond to the electric field because $\Delta\epsilon$ is negative. In the low-frequency regime where $f\ll f_c$, diffraction also disappears because all the LCs (no matter in the opaque or transparent stripes) are all reoriented by the electric field even though their threshold voltage is somewhat different. The phase difference between the adjacent pixels is so small that the phase grating vanishes. Figure 4(b) shows the diffraction patterns for the DFCL cell with 300 s UV exposure. The diffraction intensity is strong for the zeroth, \pm first, and \pm second orders and vanishes quickly after the third order. Comparing Figs. 4(a) and 4(b), we find that the higher-order patterns are more noticeable for the shorter UV exposed cell. By contrast, diffraction concentrates in the lower orders for the cell with a longer UV exposure.

To understand the physical mechanism of the DFCL phase grating, we have performed computer simulations of

the device structures. For a beam passing through a uniaxial LC, the accumulated phase is related to the birefringence, molecular tilted angle, cell gap, and wavelength. For a given LC material and device, the only variable is the molecular tilt angle which is determined by the voltage. By tuning the applied voltage V and frequency f of the electric field, the LC director reorientation can be calculated. For a LC phase grating, it is necessary to calculate the spatial phase difference. After a laser beam traverses a homogeneous LC cell, the phase retardation δ (in the small angle regime) is equal to¹¹

$$\delta = \delta_{\max} \frac{\left[\left(\frac{n_e}{n_o} \right)^2 + \left(\frac{n_e}{n_o} \right) \right]}{\left[\frac{k_{33}}{k_{11}} + \frac{\Delta\epsilon}{(\epsilon_{\perp})_i} \right]} \left(\frac{V}{\pi \sqrt{\frac{K_{ii}}{\epsilon_o \Delta\epsilon_i}}} - 1 \right). \quad (1)$$

Here, $i=1$ stands for the unexposed pixels and $i=2$ for the exposed ones. If the spatial variation of $\Delta\epsilon(f)$ is considered,

$$\eta = \sqrt{\alpha^2 \sin^2 c^2(n\alpha) + (1-\alpha)^2 \sin^2 c^2[n(1-\alpha)] + 2\alpha(1-\alpha) \sin c(n\alpha) \sin c[n(1-\alpha)] \cos(\phi - n\pi)}. \quad (3)$$

From Fig. 1(b), we find $\alpha \sim 0.6$. Under such a condition, the peak diffraction efficiency reaches $\eta \sim 0.6$, which agrees well with the experimental data ($\eta \sim 0.59$). From theory, the highest diffraction efficiency occurs at $\alpha=0.5$, i.e., equal

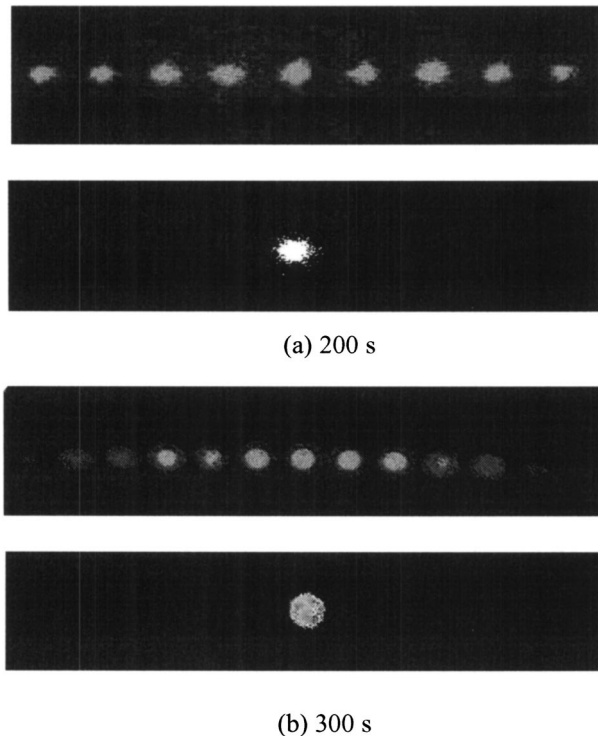


FIG. 4. Diffraction patterns of the DFLC cell after (a) 200 s and (b) 300 s UV exposure. The UV illumination is through a photomask. The single spot photos represent the nondiffraction stage at $f > f_c$. The applied voltage is fixed at $30 V_{\text{rms}}$; $T=23^\circ\text{C}$ and $\lambda=633\text{ nm}$.

the amplitude distribution U with phase difference ϕ between the opaque and transparent pixels can be described as:¹²

$$U = \left\{ \text{rect} \left(\frac{x - \frac{(\alpha)P}{2}}{(\alpha)P} \right) \times e^{-i\phi} + \text{rect} \left(\frac{x - \frac{(1-\alpha)P}{2}}{(1-\alpha)P} \right) \right\} \cdot \frac{1}{P} \text{comb} \left(\frac{x}{P} \right), \quad (2)$$

where P is the period of the photomask and α is the percentage of the opaque area of the grating. Taking the Fourier transform of Eq. (2), the diffraction efficiency (η) of the n th order has the following form:

opaque and transparent pixel size. This result is important for designing the photomask patterns for optimizing the grating performance.

In conclusion, we demonstrate a frequency controlled diffraction phase grating based on the selected UV-induced polymerization in a DFLC cell. The measured first-order diffraction efficiency reaches $\sim 60\%$. Simulation results agree well with experiments. Potential applications of such a device are for laser beam steering and an imaging system where low cost, low applied voltage, and fast response time are critical.

This work is supported by AFOSR under Contract No. F49620-01-1-0377.

¹P. F. McManamon, T. A. Dorschner, D. L. Corkum, L. Friedman, D. S. Hobbs, M. Holz, S. Liberman, H. Q. Nguyen, D. P. Resler, R. C. Sharp, and E. A. Watson, Proc. IEEE **84**, 268 (1996).

²H. Ren, Y. H. Fan, and S. T. Wu, Appl. Phys. Lett. **82**, 3168 (2003).

³D. V. Wick, T. Martinez, S. R. Restaino, and B. R. Stone, Opt. Express **10**, 60 (2002).

⁴C. M. Titus and P. J. Bos, Appl. Phys. Lett. **71**, 2239 (1997).

⁵H. Ren and S. T. Wu, Appl. Phys. Lett. **81**, 3537 (2002).

⁶S. W. Kang, S. Sprunt, and L. C. Chien, Appl. Phys. Lett. **78**, 3782 (2001).

⁷H. K. Bucher, R. T. Klingbiel, and J. P. VanMeter, Appl. Phys. Lett. **25**, 186 (1974).

⁸J. Thisayukta, T. Masumi, Y. Shiraishi, N. Toshima, S. Kobayashi, A. Sawada, and S. Naemura, Soc. Information Display Tech. Digest **34**, 696 (2003).

⁹P. T. Lin and S. T. Wu, Mol. Cryst. Liq. Cryst. **411**, 243 (2004).

¹⁰H. Ren, Y. H. Fan, S. Gauza, and S. T. Wu, Opt. Commun. **230**, 267 (2004).

¹¹I. C. Khoo and S. T. Wu, *Optics and Nonlinear Optics of Liquid Crystals* (World Scientific, Singapore, 1993), Chap. 2.

¹²J. W. Goodman, *Introduction to Fourier Optics*, 2nd ed. (McGraw-Hill, New York, 1996), Chap. 3.